Optimization Design and Comprehensive Evaluation of Screw Contact of Space Battery Based on ANSYS

*WANG Ziquan**, *HUANG Wei*, *CHEN Weinan*, *GAO Xuefeng*, *LIN Yingjie*, *CAO Jinghua*, *YAO Zubin*

Shanghai Institute of Spacecraft Equipment, Shanghai 200240, P. R. China

(Received 24 November 2020; revised 2 February 2021; accepted 17 March 2021)

Abstract: In order to improve the safety of the battery of satellite side mounting, and prevent the screw from producing excess due to frequent assembly and disassembly, the YS-20 material replacement and structure optimization design of the screw body are carried out under the premise of not changing the original tooling. The double-shear test of YS-20 bar is carried out, and the ANSYS optimization design module is used to design $7\times7\times6$, a total of 294, calculation cases of D_1, D_2, T, the three important dimension parameters of screw structure. The actual bearing state of screw composite structure is accurately simulated by using asymmetric contact model. Three comprehensive evaluations are established, and the calculation examples satisfying the conditions are evaluated comprehensively. The final results are T=12.2 mm, D_1=16 mm, D_2=2 mm. The stress verification and contact analysis are carried out for the final scheme and the bearing state and contact state optimized screw structure are obtained.

Key words: space battery; screw; ANSYS; optimization design; contact analysis; comprehensive evaluation

CLC number: TH122 **Document code:** A **Article ID:** 1005-1120(2021)03-0474-10

0 Introduction

Screw is the key fastener of space battery, which plays a key role in the protection and support of the battery. At present, the main purpose of using nylon 1010 screw on the battery is to bear the pulling force caused by the weight of the battery, and at the same time, avoid surplus materials caused by frequent disassembly and assembly. In a large number of practical applications, nylon 1010 screw can bear the pulling force caused by the weight of the battery well. However, some types of satellites require the battery to be installed on the side. At this time, the screw mainly bears the shear force caused by the weight of the battery and the pressure on the screw surface. According to the results of simulation, it is found that the force state of nylon 1010 screw under both tension and shear force is very poor, and the maximum stress is 16 MPa and the displacement of screw composite structure is 1.104 mm. The yield strength of nylon 1010 bar is about 50 MPa, and the safety margin is very low, which cannot meet the requirement of satellite AIT (Assembly integration and test). The yield strength of polyimide plastic is about 100 MPa, which can replace the nylon 1010 rod. At the same time, the structure of the screw body can be optimized without changing the original tooling further. Before the design and optimization of polyimide screw, it is necessary to conduct shear test on this kind of YS-20 bar. The optimization design module of ANSYS can assist the simulation analysis of multi-objective and scheme[1-6]. The distribution of stress and displacement in different levels of optimization parameters

*Corresponding author, E-mail address: wangziquanringse@qq.com.

How to cite this article: WANG Ziquan, HUANG Wei, CHEN Weinan, et al. Optimization design and comprehensive evaluation of screw contact of space battery based on ANSYS[J]. Transactions of Nanjing University of Aeronautics and Astronautics, 2021, 38(3): 474-483.

http://dx.doi.org/10.16356/j.1005-1120.2021.03.011

is obtained. The contact analysis of structural assembly parts can also be carried out in ANSYS, so as to obtain the contact state and change of the contact parts. Although the optimization design exploration can give the calculation results of each example, when there are too many optimization indexes, it is impossible to give a better recommendation scheme, and the recommended scheme may not be the desired one. Therefore, some comprehensive evaluation and decision making methods should be used to assist the engineers, such as grey correlation analysis[7-12], comprehensive evaluation method based on fuzzy mathematics[13-17], etc. Feng et al.[18] introduced a new grey correlation model to analyze heterogeneous data, and proposed a comprehensive safety risk factor identification method, which was applicable to the identification of safety risk factors of heterogeneous sparse small reservoirs. Liu et al.[19] proposed a multi-level fuzzy comprehensive evaluation method, which could be used as a reference for gas enterprises to develop urban gas monitoring and data acquisition system infrastructure.

Therefore, some comprehensive evaluation and decision-making methods can be used to assist the scheme evaluation when the recommended scheme cannot be given by ANSYS or the given scheme is not desired. In this paper, three comprehensive evaluation methods: Relative deviation fuzzy matrix evaluation method, relative superior membership degree fuzzy matrix evaluation method, and variable weight grey correlation degree evaluation method, are used to conduct comprehensive evaluation and decision-making for the calculation examples. And the double shear test of YS-20 bar screw is carried out, and the shear stress of the screw is obtained. The structural optimization design of the screw based on ANSYS is carried out, and 294 kinds of calculation examples are obtained. The stress verification and contact analysis of the optimized model are carried out, and the screw structure meeting the engineering requirements is obtained.

1 Double Shear Test of YS-20 Polyimide Bar

Before designing and optimizing the polyimide screw, it is necessary to know the shear performance of the bar. Referring to the metal compression test method, the design of the test fixture is shown in Fig.1. The grade of the designed test bar is YS-20, the design diameter is 6.65 mm, and the design theoretical shear area volume is $2\times\pi\times 6.65^2$. The lower cutter is fixed on the fixed block, and the feed speed of the upper cutter is composed of four groups: 0.03, 0.3, 0.6, and 0.9 mm/min, in which the cutter feed rate is 0.03, 0.3, 0.6, and 0.9 mm/min for one time, three times, three times, and one time, respectively. The upper cutter and the fixing block are fixed on the machine frame.

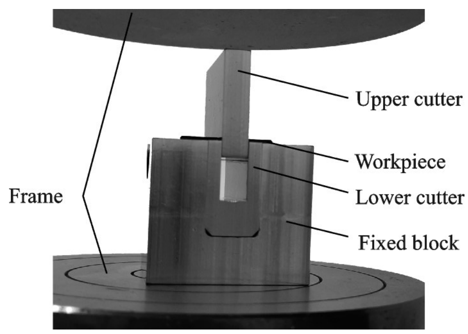

Fig.1 Shear test tooling of YS-20 polyimide bar

In the test, the bar diameter for 0.03 mm/min cutter is 6.62 mm, while those for 0.3, 0.6, and 0.9 mm/min are 6.64 mm. The maximum shear yield strength of the bar is shown in Fig.2, and the failure of the test bar when the cutter feed speed is 0.3 mm/min and 0.6 mm/min are shown in Fig.3. It

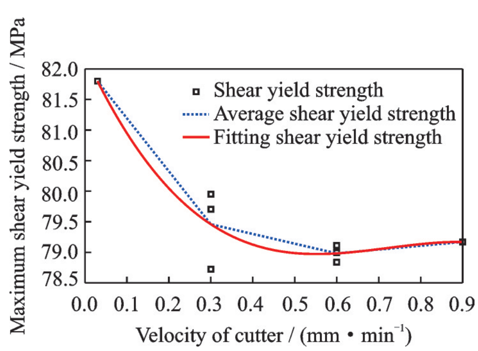

Fig.2 Maximum shear yield strength of YS-20 bar

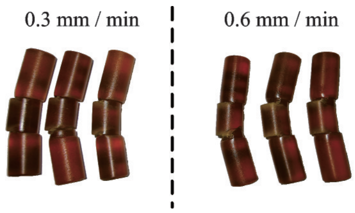

Fig.3 Shear failure of YS-20 bar

can be seen that when the rate of cutter feed is 0.03 mm/min, the maximum shear yield stress is larger, which is related to the slow feed rate. With the increase of the speed, the maximum shear yield stress decreases. But it can be seen from Fig.3 that the test bar has produced obvious fracture phenomenon, and the data point dispersion at the speed of 0.3 mm/min is larger than that of 0.6 mm/min, and the data points at the speed of 0.6 mm/min are basically unchanged, thus indicating that the test has entered the steady state region, and the maximum shear yield stress in this region can best reflect the shear strength of the material. The shear stress ranges from 78.722 7 MPa to 81.799 3 MPa. The average maximum shear yield stress of each group of tests is fitted by cubic polynomial. It can be seen that the maximum shear yield stress of cutter feed rate from 0.3 mm/min to 0.9 mm/min has been basically unchanged, and the stress change value is about 79 MPa, which is basically consistent with the actual test results. According to the fitting data, the minimum value of the maximum shear yield stress is 78.972 0 MPa.

2 Optimization Parameters of Screw and Comprehensive Evaluation

2.1 Parameters and optimization

Without changing the original tooling, the main contact and support parts of the screw are extracted as shown in Fig.4. The overall structure includes screws, nylon bushing and aluminum alloy support parts. There are eight symmetrically distributed screws in the tooling, so one screw can be calculated according to the average load in ANSYS simulation. According to the structural model, the

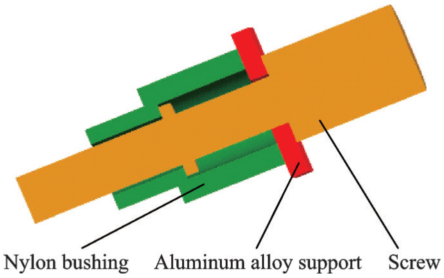

Fig.4 Screw and its combination structure

ANSYS simulation model is established. It can be seen that the structure has two support surfaces Ⅰ and Ⅱ, and six groups of contact pairs, as shown in Fig.5. In the simulation model, the friction coefficient is 0.2, the normal stiffness factor of the contact surface is 0.1, the contact method is asymmetric, and the tension and the shear force of the screw surface are F_l=60 N and F_y=60 N, respectively. Set three optimization parameters (unit: mm): D_1 the diameter of the Ⅱ supporting surface; D_2 the axial gate thickness of Ⅰ and Ⅱ; and T the diameter of the Ⅰ supporting surface. There are seven optimization levels for the optimization parameter D_1, six optimization levels for T, seven optimization levels for D_2, and 294 for each parameter level in ANSYS optimization design.

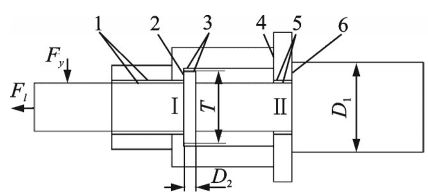

Fig.5 Optimizing parameters

The mesh division of the screw composite structure is shown in Fig.6. The mesh of the surface fixed on the ground can be roughly processed to improve the calculation efficiency. The mesh refinement treatment is carried out at the contact surface,

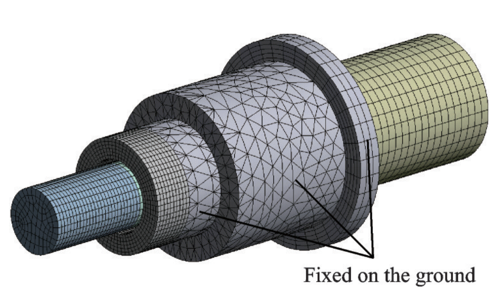

Fig.6 Mesh of screw composite structure

and the sweeping grid division is carried out for the cylindrical structure (e.g. aluminum alloy support). The average skewness of the overall structure grid is 0.224, which has a high grid quality.

2.2 Comprehensive evaluation method

The constituent factors of many decision-making problems are interrelated and mutually restricted. Some indicators are difficult to quantify and others contradict each other, resulting in the complexity of decision-making. Therefore, it is necessary to manually evaluate the calculation results or schemes.

2.2.1 Fuzzy comprehensive evaluation

Relative deviation fuzzy matrix evaluation method is a kind of fuzzy comprehensive evaluation method, which is the specific application of fuzzy mathematics. Its basic idea is: on the basis of fuzzy mathematics, using the principle of fuzzy relation synthesis, quantifying some factors with unclear boundary and difficult to quantify, and comprehensively evaluating the subordinate level of the evaluated thing from multiple factors. The basic evaluation steps are as follows:

(1) Determining evaluation index and level

Assume that $U=[u_1, u_2, \cdots, u_m]$ is the factor of the evaluation object, and the boject has m members; $V=[v_1, v_2, \cdots, v_n]$ is the evaluation level, and the evaluation level has n members.

(2) Constructing fuzzy comprehensive evaluation matrix

The membership degree r_{ij} of the evaluation index u_i can be rated as grade v_j. r_{ij} can be understood as the membership degree of index u_i to grade v_j, and it is usually used in normalization. The fuzzy comprehensive evaluation matrix is obtained as

$$\boldsymbol{R}=(r_{ij})_{m\times n}=\begin{pmatrix} r_{11} & r_{12} & \cdots & r_{1n} \\ r_{21} & r_{22} & \cdots & r_{2n} \\ \vdots & \vdots & \ddots & \vdots \\ r_{m1} & r_{m2} & \cdots & r_{mn} \end{pmatrix} \tag{1}$$

(3) Determining the weight of evaluation index

In order to obtain the weight of the index, we can use the coefficient of variation method. Firstly, we should calculate the mean and variance of the i index.

$$\begin{cases} \bar{x}_i=\dfrac{1}{n}\sum\limits_{j=1}^{n}a_{ij} \\ s_i^2=\dfrac{1}{n-1}\sum\limits_{j=1}^{n}(a_{ij}-\bar{x}_i) \end{cases} \tag{2}$$

where a_{ij} is the specific value of j in the i index.

Ordering that $v_i=s_i/\left|\bar{x}_i\right|$, the normalized v_i is the weight of each index

$$\omega_i=\frac{v_i}{\sum v_i} \tag{3}$$

(4) Fuzzy synthesis

Fuzzy comprehensive evaluation uses weight vectors to synthesize different rows, so as to obtain the overall membership degree of the evaluation objects to each level. The calculation needs to be realized by fuzzy synthesis. The operators of fuzzy synthesis are as follows

$$\begin{cases} M(\wedge,\vee): b_j=\bigvee\limits_{i=1}^{m}(a_i\wedge r_{ij}) \\ M(\cdot,\vee): b_j=\bigvee\limits_{i=1}^{m}(a_i\cdot r_{ij}) \\ M(\wedge,\oplus): b_j=\sum\limits_{i=1}^{m}(a_i\wedge r_{ij}) \\ M(\cdot,\oplus): b_j=\sum\limits_{i=1}^{m}(a_i\cdot r_{ij}) \end{cases} \tag{4}$$

In Eq.(4), getting small and large values operations are represented by $\wedge$, $\vee$, respectively.

2.2.2 Relative deviation fuzzy matrix evaluation method

Firstly, assume an ideal scheme u. Then, the weight $\boldsymbol{A}$ of each evaluation index is determined. Finally, the comprehensive distance F of each scheme is obtained by weighted average of $\boldsymbol{A}$ and $\boldsymbol{R}$, and the schemes are sorted according to the size of F. The main steps of this method are as follows:

(1) Virtual ideal scheme

$$\begin{cases} u=(u_1,u_2,\cdots,u_n) \\ u_i=\begin{cases} \max\limits_j\{a_{ij}\} & a_{ij}\text{ is benefit indicators} \\ \min\limits_j\{a_{ij}\} & a_{ij}\text{ is cost indicators} \end{cases} \end{cases} \tag{5}$$

(2) Establishment of relative deviation fuzzy matrix $\boldsymbol{R}$

The elements in $\boldsymbol{R}$

$$r_{ij}=\frac{\left|a_{ij}-u_i\right|}{\max\limits_j\{a_{ij}\}-\min\limits_j\{a_{ij}\}} \tag{6}$$

(3) Weighted averaging of deviations for each scheme

$$F_j=\sum_{i=1}^{m} w_i r_{ij} \tag{7}$$

2.2.3 Grey relational analysis

The method of judging the degree of correlation between data series based on grey correlation degree is called grey correlation analysis. Building evaluation objects and evaluation indexes which has m and n members, respectively. The signature sequence $x_0=[x_0(k)|k=1, 2,\cdots, n]$, and the related factors sequence $x_i=[x_i(k)|k=1, 2,\cdots, n]$, $i=1, 2,\cdots, m$. Order that $X_i=[x_i(1), x_i(2),\cdots, x_i(n)]$ are data sequences, $X_iD=[x_i(1)d, x_i(2)d,\cdots, x_i(n)d]$. The elements of X_iD can be obtained as follows:

Initial image

$$x_i(k)d=\frac{x_i(k)}{x_i(1)} \tag{8}$$

Mean image

$$x_i(k)d=\frac{x_i(k)}{\bar{X}_i},\ \bar{X}_i=\frac{1}{n}\sum_{k=1}^{n}x_i(k) \tag{9}$$

Interval-valued image

$$x_i(k)d=\begin{cases}\dfrac{\max\limits_k x_i(k)-x_i(k)}{\max\limits_k x_i(k)-\min\limits_k x_i(k)} & \text{Type of cost}\\[2ex] \dfrac{x_i(k)-\min\limits_k x_i(k)}{\max\limits_k x_i(k)-\min\limits_k x_i(k)} & \text{Type of benefit}\end{cases} \tag{10}$$

In order to reduce the influence of extreme values, a resolution coefficient ξ is set in the grey correlation degree, and a formula for calculating the grey correlation coefficient is obtained

$$\begin{cases}y(k)=x_0(k)-x_i(k)\\ \gamma_i(k)=\dfrac{\min\limits_i\min\limits_k\left|y(k)\right|+\xi\max\limits_i\max\limits_k\left|y(k)\right|}{\left|y(k)\right|+\xi\max\limits_i\max\limits_k\left|y(k)\right|}\end{cases} \tag{11}$$

The calculation formula of grey correlation degree can be obtained by weighted average of each grey correlation coefficient

$$\gamma_i=\sum_{k=1}^{n}\omega_k\gamma_i(k) \tag{12}$$

Grey correlation degree is an index to measure the degree of correlation between data series. The weight of each evaluation index is equal, which is $1/n$ (n is the number of indicators), and the weight of each index can also be determined according to the coefficient of variation method. It should be noted that different comprehensive evaluation methods have different ranking results for the same problem. Therefore, several comprehensive evaluation methods should be applied to evaluate a same problem at the same time in order to improve the reliability and persuasion of the evaluation results.

3 Simulation Results and Scheme Decision

3.1 Simulation results of screw composite structure

The distribution of stress, displacement and strain of the screw composite structure with the optimized parameters is obtained, as shown in Figs.7—9. It can be seen from Fig.7 that the stress of screw composite structure has obvious nonlinear change with the change of optimization parameters, and the regularity is weak, which is consistent with the actual situation. The maximum value of stress is 22.214 MPa, and the minimum value is 12.666 MPa. The regions with small stress are mainly concentrat-

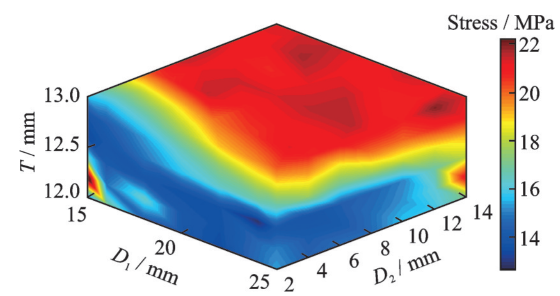

Fig.7 Stress distribution of screw composite structure

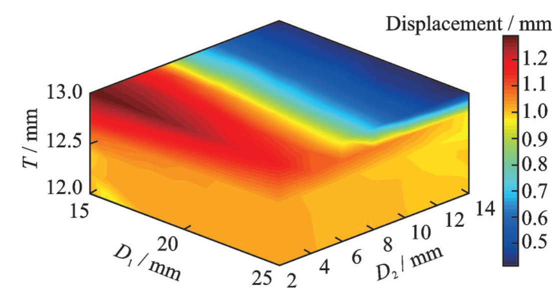

Fig.8 Displacement distribution of screw composite structure

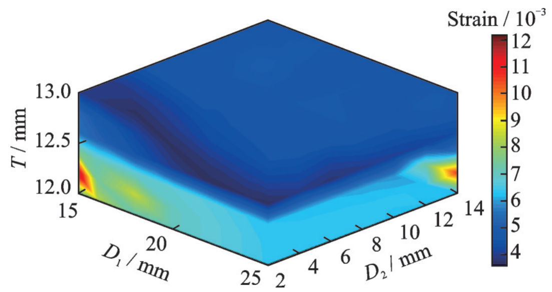

Fig.9 Strain distribution of screw composite structure

ed in the range of $T \leqslant 12.5$ mm, $D_1 \geqslant 16$ mm, $D_2 \leqslant 12$ mm, and the comprehensive evaluation results are the most likely to fall into these regions.

It can be seen from Fig.8 that the displacement distribution of screw composite structure is nonlinear and the regularity is weak. The maximum displacement value is 1.291 mm, and the minimum value is 0.413 mm. The regions with small displacement are mainly concentrated in the range of $T \geqslant 12.5$ mm, $D_1 \geqslant 15$ mm, $D_2 \geqslant 8$ mm. At the level of $T = 13$ mm, $D_2 = 8$ mm is the boundary layer. When $D_2 > 8$ mm, the displacement decreases with the increase of D_2, and when $D_2 \leqslant 8$ mm, the displacement increases with the decrease of D_2. Therefore, the displacement has a strong linear law in some local regions. It can be seen from Fig.9 that the strain distribution of the screw composite structure is nonlinear, and the maximum strain is 0.012 2 and the minimum strain is 0.003 6. The region with small strain is mainly concentrated in the range of $T \geqslant 12.5$ mm, and $T = 12.5$ mm is the boundary layer with obvious strain distribution.

The distribution of stress, displacement and strain of the screw structure with the optimized parameters is obtained, as shown in Figs. 10—12. It can be seen from Fig.10 that the stress of screw structure has obvious nonlinear change with the change of optimization parameters, and the regulari-

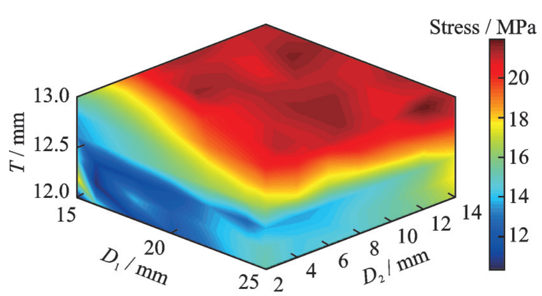

Fig.10 Stress distribution of screw structure

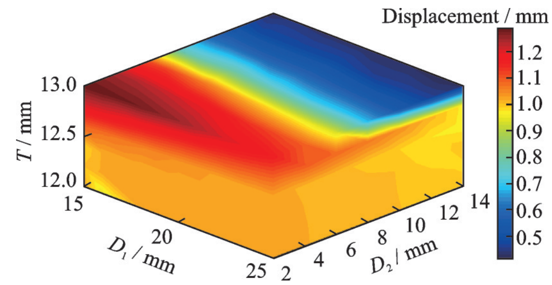

Fig.11 Displacement distribution of screw structure

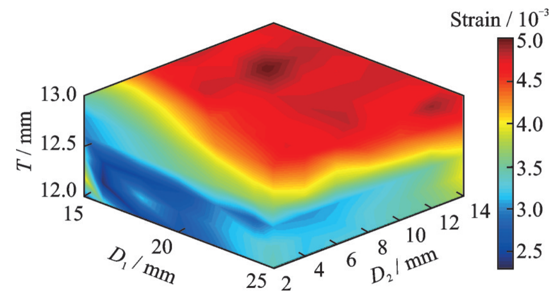

Fig.12 Strain distribution of screw structure

ty is weak, which is consistent with the actual situation. The maximum stress is 21.972 MPa and the minimum is 10.326 MPa. The smaller stress regions are mainly concentrated in the range of $T \leqslant 12.5$ mm, $D_1 \geqslant 16$ mm, $D_2 \leqslant 12$ mm.

It can be seen from Fig.11 that the displacement distribution of the screw structure is nonlinear, and the maximum displacement is 1.291 mm, the minimum displacement is 0.413 mm, which is the same as that of the composite structure. The smaller displacement regions are mainly concentrated in the range of $T \geqslant 12.5$ mm, $D_1 \geqslant 15$ mm, $D_2 \geqslant 8$ mm. At the level of $T = 13$ mm, $D_2 = 8$ mm is the boundary layer of this level. It can be seen from Fig. 12 that the strain distribution of screw structure is nonlinear, the maximum strain value is 0.005 and the minimum value is 0.002 3, and the regions with small strain are mainly concentrated in the range of $T \leqslant 12.5$ mm, $D_1 \geqslant 16$ mm, $D_2 \leqslant 10$ mm.

3.2 Comprehensive evaluation and decision-making

According to the simulation results, nine parameters of screw structure size T, D_1, D_2, stress, displacement and strain of screw composite structure and screw stress, displacement and strain are taken as optimization indexes. The nine parameters selected are all cost indicators. The F distribution of each evaluation method with the optimization parameters is obtained as shown in Figs.13—15. According to Fig.13, the F distribution changes at different levels with the change of optimization parameters. The regions with smaller F value are mainly concentrated in the range of $T \leqslant 13$ mm, $D_1 \geqslant 15$ mm, $D_2 \leqslant 4$ mm, the minimum value of F is 0.185 9, and the corresponding optimization parameter value is $T = 12.2$ mm, $D_1 = 16$ mm, $D_2 = 2$ mm.

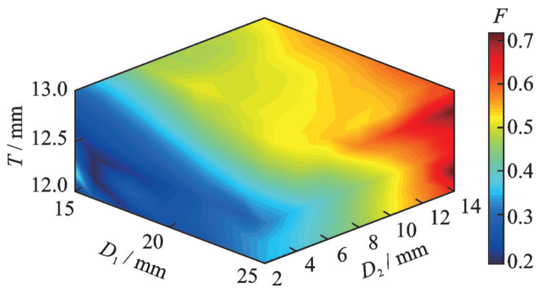

Fig.13 F distribution of fuzzy matrix evaluation method with relative deviation

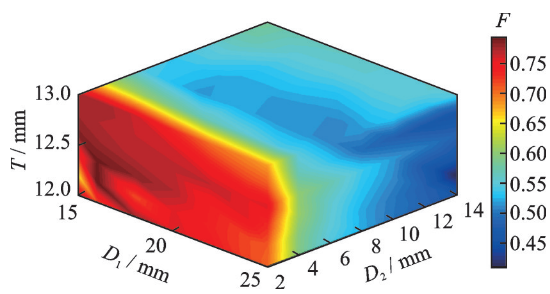

Fig.14 F distribution of fuzzy matrix evaluation method with relative superior membership degree

According to Fig.14, the regions with smaller F values are mainly concentrated in the range of $T \leqslant 13$ mm, $D_1 \geqslant 15$ mm, $D_2 \leqslant 3$ mm, the maximum value of F is 0.795 14, and the corresponding optimization parameter values are $T = 12.2$ mm, $D_1 = 16$ mm, $D_2 = 2$ mm.

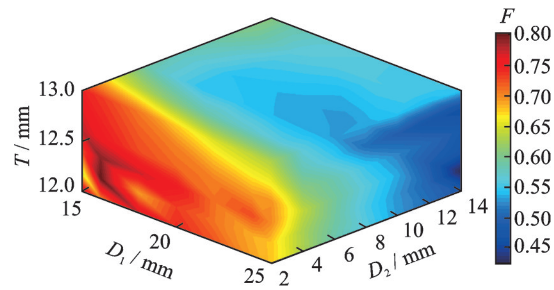

Fig.15 F distribution of variable weight grey correlation evaluation method

According to Fig. 15, the regions with smaller F values are mainly concentrated in the range of $T \leqslant 13$ mm, $D_1 \geqslant 15$ mm, $D_2 \leqslant 3$ mm, the maximum value of F is 0.804 3, and the corresponding optimization parameter values are $T = 12.2$ mm, $D_1 = 16$ mm, $D_2 = 2$ mm.

Take the six top schemes of the three evaluation methods to get the F ranking and corresponding optimization parameter values, as shown in Table 1. It can be seen that the optimal schemes obtained by the three evaluation methods are all $T = 12.2$ mm, $D_1 = 16$ mm, $D_2 = 2$ mm. The F values of the first two schemes of the relative deviation fuzzy matrix evaluation method and the relative superior membership degree fuzzy matrix evaluation method are not significantly different, so the scheme with $T = 12.4$ mm, $D_1 = 16$ mm, $D_2 = 2$ mm can also be considered.

Table 1 *F* ranking of evaluation methods and corresponding optimization parameter values

Relative deviation fuzzy matrix evaluation method		Fuzzy matrix evaluation method of relative superior membership degree		Variable weight grey correlation evaluation method	
F	Value	F	Value	F	Value
0.185 9	[12.2, 16, 2]	0.795 1	[12.2, 16, 2]	0.804 2	[12.2, 16, 2]
0.191 1	[12.4, 16, 2]	0.792 3	[12.4, 16, 2]	0.794 6	[12.0, 15, 2]
0.191 6	[12.0, 15, 2]	0.786 0	[12.6, 15, 2]	0.793 0	[12.4, 16, 2]
0.208 6	[12.0, 18, 2]	0.783 4	[12.0, 15, 2]	0.776 7	[12.6, 15, 2]
0.210 2	[12.4, 18, 2]	0.782 7	[12.4, 18, 2]	0.774 6	[12.0, 18, 2]
0.216 1	[12.0, 15, 4]	0.778 5	[12.0, 18, 2]	0.771 6	[12.4, 18, 2]

4 Structural Verification and Contact Analysis

Taking the optimal scheme $T = 12.2$ mm, $D_1 = 16$ mm, $D_2 = 2$ mm, the structural verification and contact state analysis are carried out in ANSYS, and the stress verification of screw composite structure and screw is obtained, as shown in Fig.16.

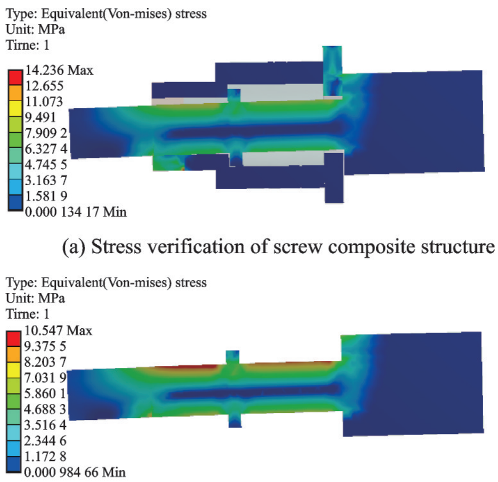

(a) Stress verification of screw composite structure

(b) Stress calibration of screw structure

Fig.16 Screw composite structure and screw stress verification

It can be seen that the maximum stress of screw composite structure is 14.236 MPa, which is nearly 2 MPa less than that before optimization, and the maximum stress of screw body structure is 10 MPa. At the same time, the bearing capacity of the screw is significantly improved compared with that before optimization, which meets the expectation of optimal design.

The contact state of screw composite structure is obtained as shown in Fig.17. It can be seen from Fig.17(a) that the contact state of some contact areas of 1, 2, 4 and 6 contact pairs of the composite structure is embedded, which corresponds to the

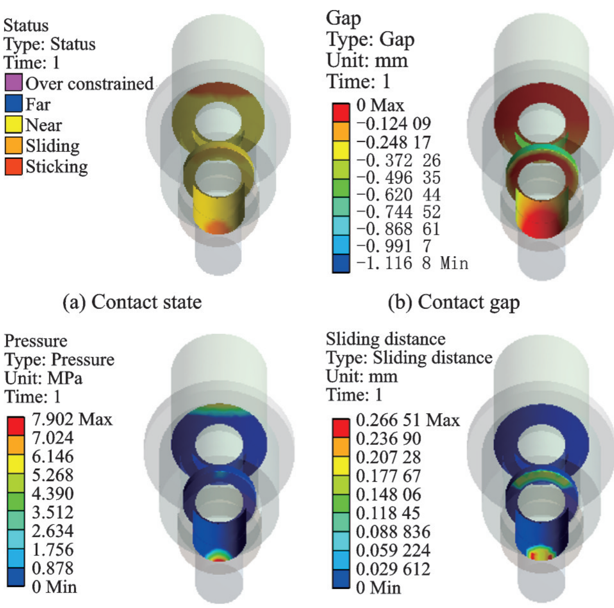

(a) Contact state (b) Contact gap

(c) Contact pressure (d) Sliding distance

Fig.17 Contact state of screw composite structure

magnitude and direction of the force on the structure, indicating that the materials in this part of the region have large contact pressure, which results in the mutual embedding of materials. The other contact surfaces are basically sliding or close, such as the contact surfaces corresponding to contact pair 3 and contact pair 5. According to the contact gap shown in Fig.17(b), the contact state between contact pairs can be further understood. The contact gap of contact pair 3 and contact pair 5 is about 0.5 mm, which is close to the contact state. Fig.17(c) shows the contact pressure distribution of each contact surface. The contact pressure of the embedded contact surface is larger, and the maximum contact pressure appears on contact pair 1 and it is 7.902 MPa, corresponding to the magnitude and direction of the stress on the structure. According to the contact slip situation in Fig.17(d), the sliding distance of contact surface corresponding to contact pairs 1 and 3 is relatively large. The main reason is that the screw moves along the radial direction after being stressed, resulting in the larger sliding distance of contact surface corresponding to contact pair 3. At the same time, the cylinder surface of the screw head is in contact with the nylon bushing, resulting in larger contact pressure and a larger sliding distance in some regions of the contact surface. Comprehensive analysis shows that the contact state of screw composite structure under the design load is in line with the actual change.

5 Conclusions

The material substitution and structural contact optimization design of a load-bearing screw of space battery are studied. The double shear test of YS-20 bar is carried out, and the maximum shear stress is obtained, which verified the possibility of replacing nylon 1010. Without changing the original tooling, the screw structure is optimized and 294 schemes are obtained. The final scheme is obtained by using three comprehensive evaluation methods. The stress verification and contact analysis of the final scheme show that the comprehensive stress and shear stress meet the requirements. The screw can bear the weight of the battery body well in actual use, and can continue to be used after several working cycles. It has strong anti-fatigue performance and long service life.

References

[1] QI Xiaodong, SHEN Xiuli. Multidisciplinary design optimization of turbine disks based on ANSYS workbench platforms[J]. Procedia Engineering, 2015, 99: 1275-1283.

[2] MAHERI A. Multiobjective optimization and integrated design of wind turbine blades using WTBM-ANSYS for high fidelity structural analysis[J]. Renewable Energy, 2020, 145: 814-834.

[3] KUMAR P, MATAWALE C R. Analysis and optimization of mono parabolic leaf spring material using ANSYS[M]. Materials Today: Proceedings, 2020.

[4] JANKOVICS D, GOHARI H, TAYEFEH M, et al. Developing topology optimization with additive manufacturing constraints in ANSYS[J]. IFAC-PapersOnLine, 2018, 51(11): 1359-1364.

[5] CHEN Y, ZHU F. The finite element analysis and the optimization design of the Yj3128-type dump truck's sub-frames based on ANSYS[J]. Procedia Earth and Planetary Science, 2011, 2: 133-138.

[6] JIA Wenbin, WEN Weidong, FANG Lei. Damage initiation and propagation in composites subjected to low-velocity impact: Experimental results, 3D dynamic damage model, and FEM simulations[J]. Transactions of Nanjing University of Aeronautics and Astronautics, 2019, 36(3): 488-499.

[7] XIE W, MA Y, LI S, et al. Optimizing soil dissolved organic matter extraction by grey relational analysis[J]. Pedosphere, 2020, 30(5): 589-596.

[8] GUGULOTHU B, RAO G K M, BEZABIH M. Grey relational analysis for multi-response optimization of process parameters in green electrical discharge machining of Ti-6Al-4V alloy[J]. Materials Today: Proceedings, 2020. DOI: https://doi.org/10.1016/j.matpr.2020.06.135.

[9] SUN X, HU Z, LI M, et al. Optimization of pollutant reduction system for controlling agricultural non-point-source pollution based on grey relational analysis combined with analytic hierarchy process[J]. Journal of Environmental Management, 2019, 243: 370-380.

[10] YANG Bo, WANG Xingdong, KONG Jianyi, et al. Modeling and optimal design of planar linkage mechanism of coupled joint clearances for manufacturing[J]. Transactions of Nanjing University of Aeronautics and Astronautics, 2018, 35(4): 719-728.

[11] ZHANG H, HE X q, MITRI H. Fuzzy comprehensive evaluation of virtual reality mine safety training system[J]. Safety Science, 2019, 120: 341-351.

[12] YU H Y, CHEN Y L, WU Q, et al. Decision support for selecting optimal method of recycling waste tire rubber into wax-based warm mix asphalt based on fuzzy comprehensive evaluation[J]. Journal of Cleaner Production, 2020, 265: 121781.

[13] WU X, HU F. Analysis of ecological carrying capacity using a fuzzy comprehensive evaluation method[J]. Ecological Indicators, 2020, 113: 106243.

[14] HE Z, LI M, CAI Z, et al. Optimal irrigation and fertilizer amounts based on multi-level fuzzy comprehensive evaluation of yield, growth and fruit quality on cherry tomato[J]. Agricultural Water Management, 2021, 243: 106360.

[15] DU Y W, WANG S S, WANG Y M. Group fuzzy comprehensive evaluation method under ignorance[J]. Expert Systems with Applications, 2019, 126: 92-111.

[16] NGA T T V, NAM P T, NAM H N. Adaptive neuro-fuzzy inference system based path planning for excavator arm[J]. Journal of Robotics, 2018, 2018: 2571243-2571247.

[17] LIU Kuo, GUO Dameng, LIU Jie, et al. Research and simulation of hydraulic excavator's adaptive fuzzy sliding control[J]. Journal of Northeastern University, 2009, 30(11): 1649-1652.

[18] FENG J C, HUANG H A, YIN Y, et al. Comprehensive security risk factor identification for small reservoirs with heterogeneous data based on grey relational analysis model[J]. Water Science and Engineering, 2019, 12(4): 330-338.

[19] LIU W, HUI L, LU Y, et al. Developing an evaluation method for SCADA-controlled urban gas infrastructure hierarchical design using multi-level fuzzy comprehensive evaluation[J]. International Journal of Critical Infrastructure Protection, 2020, 30: 100375.

Author Mr. **WANG Ziquan** received the B.S. and M.S. degrees in mechanical engineering and automation from Anhui University of Science and Technology, Huainan, China, and mechanical designing and automation from Hefei University of Technology, Hefei, China, in 2017 and 2020, respectively. From 2020 to present, he has been with the Satellite AIT Center, Shanghai Institute of Spacecraft Equipment, where he is currently a full production engineer.

His research has focused on mechanical and electronic engineering, embedded system development technology, hydraulic and pneumatic engineering.

Author contributions Mr. **WANG Ziquan** designed the study, complied the models, and conducted the analysis. Miss. **HUANG Wei**, Mr. **CHEN Weinan**, and Mr. **GAO Xuefeng** designed the experimental model. Mr. **LIN Yingjie**, Mr. **CAO Jinghua**, and Mr. **YAO Zubin** conducted the experimental verification. All authors commented on the manuscript draft and approved the submission.

Competing interests The authors declare no competing interests.

(Production Editor: XU Chengting)

基于ANSYS的空间电池装星螺钉接触优化设计与综合评价

王子权，黄　巍，陈伟男，高雪峰，林颖杰，曹敬华，姚祖斌

（上海卫星装备研究所，上海 200240，中国）

摘要：为提高空间电池侧身装星时的安全性，防止螺钉因频繁拆装而产生多余物，针对目前空间电池某承载螺钉，在不改变原工装前提下进行了螺钉本体的YS-20型棒料代替与结构优化设计。对YS-20棒料进行了双剪切试验，采用ANSYS对螺钉结构中的3个重要尺寸参数D_1、D_2、T进行了$7\times7\times6$共294个算例水平的设计探索，采用非对称接触模型准确地模拟了螺钉组合结构的实际承载状态。通过3种综合评价方法对满足条件的算例进行了综合评价，得出T=12.2 mm，D_1=16 mm，D_2=2 mm为最终方案，对最终方案进行了应力校验与接触分析，得到了承载状态与接触状态均有优化的螺钉结构。

关键词：空间电池；螺钉；ANSYS；优化设计；接触分析；综合评价